URSI GASS 2023, Sapporo, Japan, 19 – 26 August 2023

Parameter ranges and limitations on using gold nanoparticles for radio frequency-based hyperthermia treatment of cancer

Mariana Dalarsson*(1), Brage Bøe Svendsen(1), and Balwan Rana(1)
(1) KTH Royal Institute of Technology, Stockholm, Sweden; e-mail: mardal@kth.se

Abstract

In recent years, several researchers and research groups have proposed and studied a novel method of using gold nanoparticles (AuNPs) for radio frequency (RF) hyperthermia treatment of cancer. Such a method is occasionally described as a very promising new method for cancer treatment, without the side effects that are typical for other radiation treatments. It is well established that optical heating of AuNPs is caused by localized surface plasmon resonances. However, the physical mechanism behind RF heating of AuNP-fed biological tissue is a subject of some controversy. It is believed that the applied RF radiation drives the AuNPs into resonant oscillation, leading to relatively high dielectric losses, such that Joule and inductive heating is found to be negligible. In the present paper, we therefore perform an in-depth investigation of the parameter ranges and limitations that exist for the proposed methods of using AuNPs for RF hyperthermia treatment of cancer. Thereby, we show that a number of claims made so far about the potential of the proposed method are uncertain, and require further quantitative investigation.

1 Introduction

Several researchers and research groups [1–4] have proposed using AuNPs for RF-hyperthermia based cancer treatment. The underlying theory is based on [1], while further detailed investigations are reported in [2, 3]. In [1], it was observed that the induced electric dipoles and the electric double layer surrounding each AuNP could induce an additional absorption, but that this was small compared with the absorption of the host medium. The ionic contribution from the weak electrolyte solution was found to have a more significant impact than that of the AuNPs, but did not rule out entirely the possible contribution from the motion of charged nanoparticles for the observed heating.

The source of heating of AuNPs under RF radiation is still under debate. Joule heating has been largely discarded [1, 5], although a recent paper demonstrates theoretically that significant Joule heating may occur for extremely elongated particles [6]. Recent investigations into whether heating is produced by the presence of AuNPs [7–9] or solely due to the absorbing tissue [10, 11] show conflicting conclusions.

In the present paper, we investigate the current situation regarding the Drude permittivity describing gold nanoparticles in electrophoretic motion. In our previous work [12, 13], some steps were taken to approach more realistic parameter values describing biological tissues as the host medium, instead of an electrolyte water solution used in the previous studies.

Where relevant, we have focused on literature investigating breast tissue and breast tumors. This is due to it being more likely to find studies on breast cancer, as it is one of the most common types of cancers. The physical properties may also differ between types of cancers, so it is a conscious decision to focus on one type at this stage when investigating realistic parameter values. Another assumption, motivated by limiting the scope of this paper and removing a degree of freedom, is to set the AuNP size to 5 nm. This value was chosen due to the AuNPs being able to pass through the kidneys at this dimension [14].

2 Electrophoretic heating

The electrophoretic mechanism is assumed to be described by the following relative permittivity function [1]

$$\varepsilon_r(\omega) = -\frac{\omega_p^2\tau^2}{1+\omega^2\tau^2} - \mathrm{i}\frac{\omega_p^2\tau}{\omega(1+\omega^2\tau^2)}, \qquad (1)$$

where $\omega_p^2 = \sigma/(\varepsilon_0\tau)$ is the plasma frequency, wherein the Drude parameters may describe an electrophoretic mechanism with static conductivity $\sigma = \mathscr{N}q^2/\beta$ and relaxation time $\tau = m/\beta$. Here, $\mathscr{N}$ is the number of charged particles per unit volume, q the particle charge, m the mass of the particle, and β the friction constant of the host medium, see [1]. The friction constant is given by Stokes' law $\beta = 6\pi\mu_f R_{\mathrm{AuNP}}$, with μ_f being the dynamic shear viscosity of the host medium and R_{AuNP} the total radius of a AuNP consisting of a gold nanoparticle core plus ligands.

In [1], the main result supporting the electrophoretic mechanism assumes an electrolyte aqeuous solution with low viscosity ($\mu_f = 10^{-3}$) and high particle volume concentration ($\phi = 2\cdot 10^{-2}$), compared to equivalent values expected for tissues. On the other hand, [1] assumes each AuNP consists of only gold cores, resulting in lower particle charge compared to AuNPs with ligands. Using rough

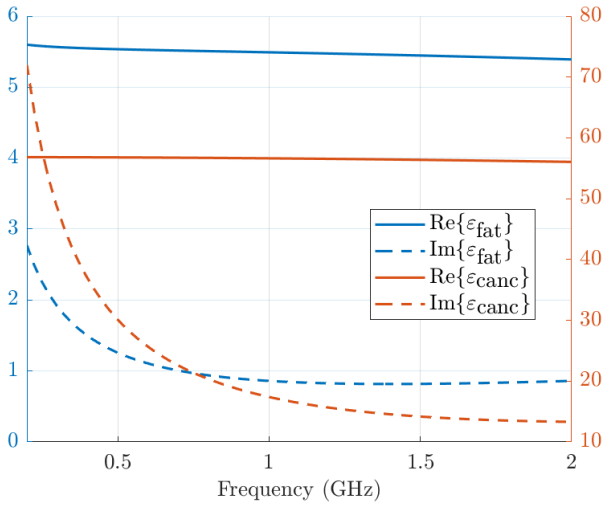

Figure 1. Dielectric permittivities of breast fat [15] and breast cancer [16].

estimates for tissue permittivity, they report that the attenuation caused by the colloidal AuNPs is 50 times smaller than the attenuation produced by the surrounding tissue. Here, we present a more thorough investigation into the ranges and limitations of the parameters of (1) better related to clinical scenarios.

The magnitude of the dielectric loss factor in the Drude permittivity of AuNPs in electrophoretic motion has been found to be low-valued compared to relevant tissues. Figure 1 shows typical values for permittivities for breast fat and breast cancer tissues. The permittivity of breast cancer tissue is significant compared to both the Drude permittivity and the surrounding breast fat tissue. In [1], a similar observation is made in their investigation of the RF absorption by tissues: the absorption in soft tissues is primarily due to the tissue conductivity, and not produced by the AuNPs.

3 Fluid mechanics of nanoparticles in biological tissue

Shear viscosity in breast cancer tissue

The viscosity of the AuNP host medium is related to (1) via Stokes' law

$$\beta = 6\pi\mu_f R_{\text{AuNP}} \tag{2}$$

While other studies have approximated the host medium as an electrolyte aqeuous solution, the host medium is expected to have a much higher viscosity in a clinical setting. Here, we discuss the shear viscosity of breast tumor as reported in two studies [17, 18].

In [17], the viscoelastic shear properties of in vivo breast lesions are measured by magnetic resonance elastography (MRE). An average shear viscosity $\mu_f = 2.4 \pm 1.7$ Pa·s is concluded, but the measured values are distinctively assorted into two different types of malignant tissue, of either low or high valued μ_f, i.e. no data points had values around the average 2.4 Pa·s. However, this value has been used in at least two other articles in their calculations [19]. Two types of breast cancer is concluded: one strongly viscous and one similar to surrounding tissue. On average, breast cancer is 4.4 ± 3.2 times more viscous than surrounding breast tissue.

In [18], the feasibility of exploiting viscoelastic parameters to differentiate between malignant and benign breast masses, as a diagnostic tool, is investigated. The values of μ_f are calculated differently than in [17], where MRE was used. An acoustic radiation force is employed to generate a push inside the soft tissue, which generates a shear wave propagating inside the medium. The method is called shear wave dispersion ultrasound vibrometry (SDUV), where the measured shear wave speed is curve-fitted to the Voigt model expression, giving a value to the shear viscosity.

Both [17] and [18] agree that malignant masses has the highest median value for shear viscosity, followed by benign and normal tissue, respectively. Both studies also agree that the distribution of shear viscosity is very broad. This implies that some malignant masses might be more viscous than others, and that different breast cancer pathologies might have different viscosity.

It is important to note, as the authors in [18] state in their article, that it is not feasible to compare the numerical values of viscosity estimated from the MRE based study [17] to the study in [18]. This is due to that the excitation frequency in MRE was limited to a single frequency, 65Hz, while in [18] all frequencies between 50-400 Hz (acoustic waves) were used. However, the values from both studies show the same trend with respect to pathology.

The two studies do not necessarily help us decide on a numerical value for shear viscosity, but rather seem to further complicate the matter. The values vary from as low as 0.7 to as high as 11.5 Pa·s. One study's higher end of standard deviation barely reaches the other study's lower end. Additionally, [18] claims that the numerical quantity in [17] (2.4 ± 1.7 Pa·s) is reliable only at a single acoustic-wave frequency due to the method of measurement. At the same time, [18] emphasises that their own values reported are "not an estimation of the ground truth, but an estimation of shear elasticity and viscosity based on the Voigt model". In summary, the two articles are highly informative on the qualitative properties of viscosity in various breast tissues, but it is still difficult to conclude on any quantitative value.

Discussion of the Stokes' law

Stokes' law (2) is used to describe the frictional force of nanoparticles in a viscoelastic tissue [20–22], where the spherical particles in the limit of low Reynolds number (laminar flow) are assumed. For fluid particles, Stokes' law holds almost exactly for Reynold's numbers (Re) below 0.1 [23], where

$$\text{Re} = \frac{\rho v_0 L}{\mu_f} \tag{3}$$

Here ρ is the mass density of the fluid, v_0 is the flow velocity, and L is the linear dimension of the particle. For electrophoretic motion of AuNPs in a biological tissue, the velocity is given by $v = v_0 e^{i\omega t}$ with amplitude

$$v_0 = \frac{qE_0}{\beta}\frac{1}{1+i\omega\tau}. \quad (4)$$

Even with the most pessimistic parameter values here, the Reynolds number (3) is of the order $\mathrm{Re} \sim 10^{-8}$, which is well below the limit 10^{-1}, such that (2) can be assumed to be accurate.

4 Nanoparticle charge

According to [24], for a colloidal suspension of AuNPs, the number n_{Au} of excess surface charge on the gold core depends on the core radius R_{Au}

$$n_{\mathrm{Au}}(R_{\mathrm{Au}}) \approx 3\cdot 10^{-9}\mathrm{m}^{-1}R_{\mathrm{Au}} + 0.5\cdot 10^{-18}\mathrm{m}^{-2}R_{\mathrm{Au}}^2 \quad (5)$$

when excluding the charge due to the ligand coating. For colloidal metal particles prepared by chemical reduction of the metal from a salt solution, it is observed that the sign of the charge depends on the element (negative for Au). The excess free charges $n_{\mathrm{Au}}q$ on the surface of the AuNP gold cores in an electrolyte solution are compensated by a countercharge of equal magnitude and opposite sign, due to ions in the electrolyte. Since charge enters the electrophoretic permittivity (1) as q^2, the sign of the charge has no consequence.

The total charge of a ligand-coated AuNP is assumed to be $q = n_{\mathrm{Au}}e_0 + n_L e_0$, where the molecular composition of ligands affect their electron count n_L. Quantitative understanding and control of charge number distribution of gold nanoparticles coated with organic ligands is challenging, see [8]. The charge with respect to the ligand shell is an important parameter in electrophoretic heating, but it is not yet fully understood how to model, measure or control it [25]. The parameter n_L is therefore not sufficiently well-understood in the literature. For example, when the charge density on a nanoparticle is $\sim 5\ e_0/\mathrm{nm}^2$, the total charge of a spherical AuNP, with radius 2.5 nm, is approximately $400e_0$ [26]. Figure 2 shows ε_r as a function of the ligand-charge count in the range $10^1 - 10^3$.

5 Particle volume concentration

The number $\mathcal{N}$ of AuNPs in a cancer cell can be expressed in terms of the particle volume concentration ϕ and the total AuNP volume V_p, as $\mathcal{N} = \phi/V_p$. Therefore, the same value of $\mathcal{N}$ can correspond to different ϕ for different V_p. In Figure 3 of [1], the attenuation produced by 5 nm radii AuNPs in a weak electrolyte aqueous dispersion is plotted, using particle volume concentrations $\phi = 2\cdot 10^{-4}, 2\cdot 10^{-3}, 2\cdot 10^{-2}$, which correspond to particle concentrations $\mathcal{N} = 0.64, 6.4, 64\ \mu\mathrm{mol}/l$. These

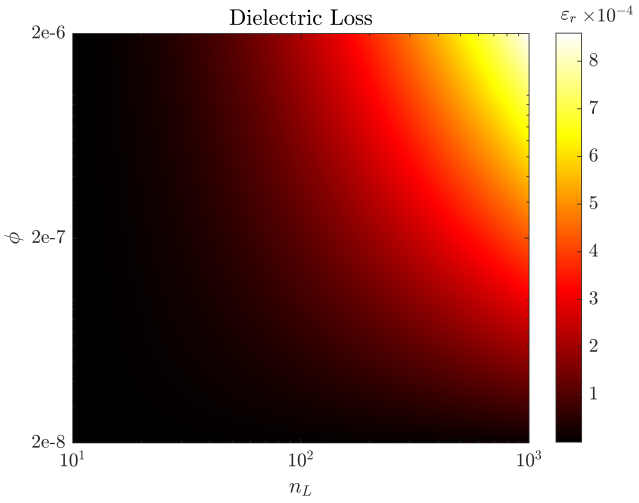

Figure 2. Electrophoretic Drude permittivity as function of ligand charge n_L and particle volume concentration ϕ at frequency 500 MHz.

values were chosen due to being in similar range as experimentally observed concentrations heated in an aqueous dispersion by RF fields [4]. However, these values do not take into account the safety limits of toxicity related to the biodistribution. Such a limit has been suggested to be around 100 μg/ml [10], which corresponds to approximately $\phi = 2\cdot 10^{-6}$ for a 5 nm size AuNP including a ligand coating and a small gold core. Figure 2 illustrates the dependency of ε_r on particle consentration ϕ, up to the supposed safety limit.

6 Discussion

In Figure 2, we have plotted the imaginary part of (1) for fixed AuNP size of 5 nm, consisting of a ligand shell with the mass density of water and a Au core of 0.75 nm, as in [2]. Keep in mind that the size of the gold nanoparticle is not only important in terms of the particle charge, frictional force, and particle concentration, but also for the biodistribution and tumor uptake [27]. In Figure 2, we assumed an optimistic scenario where the tumor has the lowest observed viscosity, $\mu_f = 0.7$ Pa·s. The dielectric loss is observed to be small, except for very high electron count in the ligand shell combined with high particle concentrations. However, the relative permittivity is still very low, compared to the relevant tissues in Figure 1. Adipose tissues such as breast fat have perhaps the lowest expected magnitude for relative permittivity in human tissues [15, 28], and (1) is here several orders of magnitude lower. These observations agrees with [1, 10, 11] that the observed produced heat is low compared to the surrounding tissue. On the other hand, there are both theoretical and experimental studies observing heat production in RF in the presence of AuNPs [2, 4, 7, 8] which suggests that the process is more complicated than what's described by the simple expression (1), which absolutely is the case. The heat may be produced by a collection of mechanisms [5].

We know that changing the AuNP size impacts the particle concentration and surface charge value. The ionic strength of the ligand shell may also influence the nanoparticles' hydrodynamic properties and consequently their electrophoretic mobility, see [8]. In addition, nanoparticle toxicity and the effectiveness of their surface charge have complicated relationships to the chemistry and biology in terms of for example dosage and uptake [29]. We have not considered the geometrical shapes of AuNPs, but recent studies suggest that negligible heating is observed for spherical particles [10] while ellipsoidal particles with high aspect ratios are more promising [6]. The theoretical study of the ellipsoidal nanoparticles [6] considered only single, isolated particles, but reported negligible Joule heating produced by spherical AuNPs over a wide frequency range. In [10], spherical AuNPs exposed to 27 MHz radiation were experimentally refuted as the cause of the heat production. Larger AuNPs at around 50 nm measured at 13.56 MHz show negligible heat production, shape-independence, and even tendency to protect the cancer tissue by their presence [11]. However, these studies, as well as studies that report heat production [2, 5, 7–9], all use different types of particle coatings, with a potentially major impact on particle properties such as charge, size, mass, and mobility.

7 Conclusions

In the present paper, we have performed an in-depth investigation of the parameter ranges and limitations that exist for the proposed methods of using gold nanoparticles (AuNPs) for RF hyperthermia treatment of cancer. We have shown that, based on the results of our investigation above, the claims made in a number of publications about the potential of the proposed method are uncertain and require further investigation. Such an investigation should include a study of the design parameters not covered here, i.e. the radii of AuNP gold core and ligand shell.

Furthermore, different studies use different types of ligands/coatings. Given that the ligand design and size (also gold core size) have impact on other parameters both directly and indirectly, further investigations should look into the choice of ligands and whether these choices can explain the different results observed in the literature (studies that support or question the efficiency of the electrophoretic heating mechanism). Therefore, the emphasis should be put on ligand designs and their effect on the electromagnetic properties and fluid mobility of the nanoparticles.

Acknowledgements

The work of M. D. was supported by the Swedish Research Council (VR) under project number 2018-05001.

References

1. Sassaroli, E., Li, K. C. P., *et al. J. Phys. D: Appl. Phys.* **45,** 1–15 (2012).
2. Nordebo, S., Dalarsson, M., *et al. J. Phys. D: Appl. Phys.* **50,** 1–12 (2017).
3. Dalarsson, M., Nordebo, S., *et al. J. Phys. D: Appl. Phys.* **50,** 1–8 (2017).
4. Gannon, C. J., Patra, C. R., *et al. Journal of Nanobiotechnology* **6,** 1–9 (2008).
5. Collins, C. B., McCoy, R. S., *et al. Nanoscale* **6,** 8459–8472 (2014).
6. Rommelfanger, N. J., Ou, Z., *et al. Phys. Rev. Applied* **15,** 054007 (2021).
7. Case, J., McNear, K., *et al. Beilstein Archives* (2022).
8. Collins, C. B., Tofanelli, M. A., *et al. The Journal of Physical Chemistry Letters* **9,** 1516–1521 (2018).
9. Rezaeian, A., Amini, S. M., *et al. Lasers in medical science* **37,** 1333–1341 (2022).
10. Narasimh, A. K., Chakaravarthi, G., *et al. Electromagnetic Biology and Medicine* **39,** 183–195 (2020).
11. Chen, C.-C., Chen, C.-L., *et al. ACS Applied Bio Materials* **2,** 3573–3581 (2019).
12. Svendsen, B. B., Söderström, M., *et al. Applied Sciences* **12** (2022).
13. Svendsen, B. B. & Dalarsson, M. in *2022 International Conference on Electromagnetics in Advanced Applications (ICEAA)* (2022), 040–040.
14. Longmire, M., Choyke, P., *et al. Nanomedicine* **3,** 703–717 (2008).
15. Gabriel, S., Lau, R. W., *et al. Phys. Med. Biol.* **41,** 2271–2293 (1996).
16. Lazebnik, M., Popovic, D., *et al. Physics in Medicine & Biology* **52,** 6093 (2007).
17. Sinkus, R., Tanter, M., *et al. Magnetic resonance imaging* **23,** 159–165 (2005).
18. Kumar, V., Denis, M., *et al. PLOS ONE* **13,** 1–15 (2018).
19. Alikhani, S., Ansari, M. A., *et al. Journal of Applied Physics* **126,** 174701 (2019).
20. Islam, M. A., Barua, S., *et al. BMC Systems Biology* **11** (2017).
21. Barua, D. *Journal of the Royal Society Interface* **15** (2018).
22. Rejniak, K., Estrella, V., *et al. Frontiers in Oncology* **3** (2013).
23. Rhodes, M. in *Introduction to Particle Technology* 29–49 (2008).
24. Rostalski, J. & Quinten, M. *Colloid and Polymer Science* **274,** 648–653 (1996).
25. Martin, M. N., Basham, J. I., *et al. Langmuir* **26,** 7410–7417 (2010).
26. Gupta, R. & Rai, B. *Scientific Reports* **7** (2017).
27. Varna, M., Ratajczak, P., *et al. Journal of Biomaterials and Nanobiotechnology* **3,** 269–279 (2012).
28. Gabriel, S., Lau, R. W., *et al. Phys. Med. Biol.* **41,** 2251–2269 (1996).
29. Alkilany, A. M. & Murphy, C. J. *Journal of Nanoparticle Research* **12,** 2313–2333 (2010).